RESEARCH ARTICLE

Decreasing arsenic accumulation but promoting arsenate biotransformation in *Microcystis aeruginosa* regulated by nano-Fe$_2$O$_3$

Yan Chen[1] · Zhenhong Wang[1] · Zhuanxi Luo[2] · Yao Zhao[1] · Jincong Yu[3]

Abstract

Iron oxide nanoparticles (nano-Fe$_2$O$_3$) widely distribute in waters with low toxicity to aquatic organisms. But it is unclear for nano-Fe$_2$O$_3$ to affect the fate of coexisting arsenic (As) with its bioaccumulation and biotransformation. In this study, we thus mainly investigated arsenate (As(V)) toxicity, uptake kinetics, biotransformation and subcellular distribution in *Microcystis aeruginosa* influenced by nano-Fe$_2$O$_3$. The results showed that *M. aeruginosa* was more sensitive to As(V) associated with nano-Fe$_2$O$_3$. Due to the exaggerated increase of efflux rate constants of As compared with the uptake rate constants in algal cells affected by different levels of nano-Fe$_2$O$_3$, the As(V) bioconcentration factor decreased with nano-Fe$_2$O$_3$ increasing correspondingly, indicating that As bioaccumulation was diminished by nano-Fe$_2$O$_3$. The decreased As accumulation in *M. aeruginosa* could be supported by the evidential As(V) sequestration through high adsorption of nano-Fe$_2$O$_3$, which resulted in decreasing free As level for algae uptake in media. Meanwhile, As subcellular distribution was adjusted by nano-Fe$_2$O$_3$ with decreasing in cell walls and rising in cytoplasmic organelles compared with nano-Fe$_2$O$_3$ free. As(V) reduction and methylation were enhanced with increasing nano-Fe$_2$O$_3$, stimulating by its sensitivity to the interaction of nano-Fe$_2$O$_3$ and As(V) as well as the rising level of As in cytoplasmic organelles of this algae. It is confirmed by the higher relative gene expression levels of *arsC* and *arsM* in elevated nano-Fe$_2$O$_3$. Accordingly, it is highlighted to be deserved more attention that the changing behavior of As(V) by nano-Fe$_2$O$_3$ that reduce As bioaccumulation and accelerate its biotransformation in algae in As contaminated water.

Keywords Arsenate · Subcellular distribution · Microcystins · Toxicity · Bioavailability

Introduction

Arsenic (As), cited as the most hazardous chemical substance, is immensely concerned due to its ubiquitous contamination with an exceedingly varying concentration in environments caused by anthropogenic and natural sources

✉ Zhenhong Wang
zhhwang1979@163.com

1. College of Chemistry, Chemical Engineering and Environment, Fujian Province Key Laboratory of Modern Analytical Science and Separation Technology, Key Laboratory of Pollution Monitoring and Control, Minnan Normal University, Zhangzhou 363000, China

2. College of Chemical Engineering, Huaqiao University, Xiamen 361021, China

3. Xiamen Mata Ecology Co., Ltd, Xiamen 361021, China

(Yan et al. 2015). Arsenic usually changes its forms biochemically in the surroundings with four stable oxidation states, i.e. elemental As (As^0), arsenate (As(V)), arsenite (As(III)) and arsine (As(-III)) (Miyashita et al. 2016). Inorganic As, especially As(V), is more abundantly found in aerobic and aquatic environment as a major contaminant at global scale (Hasegawa et al. 2010). Inorganic As undergoes methylation process and changes into organoarsenicals such as monomethylarsonic acid (MMA), dimethylarsinic acid (DMA), arsenobetaine (AsB), and arsenocholine (AsC) owing to microbial-mediated biotransformation (Li et al. 2019; Roy et al. 2015).

Cyanobacteria can play critical roles in As biotransformation and biogeochemical processes in diverse environment including oceans, freshwater, soil and groundwater. (Duncan et al. 2015; Maeda et al. 1990, 1993; Roy et al. 2015; Wang et al. 2015; Zhang et al. 2014). They are able to adsorb and uptake As vastly using their large specific surface area and functional groups in cell membrane, alter its valence change,

and convert it into methylation As species (Thomas et al. 2004; Yan et al. 2016). *Microcystis aeruginosa* (*M. aeruginosa*), the main contributor to serious cyanobacterial bloom, found abundantly in eutrophic freshwater systems, is highly tolerant of As in both field and laboratory settings (Che et al. 2018; Wang et al. 2013a, b; Zeng et al. 2019). Nowadays, cyanobacteria blooms, especially *Microcystis*, accompanied by As pollution are observed in many eutrophic freshwater lakes. *M. aeruginosa* rapidly increase their biomass in short periods combined with its high As toleration, making it possible to be used in As removal (Jia et al. 2018; Sulaymon et al. 2013; Wang et al. 2020).

Except for heavy metals, recent researches have shown the wide presence of various nanoparticles (NPs) in aquatic ecosystems. Iron oxide nanoparticles (nano-Fe_2O_3) are one of the most widely explored and utilized metal nanomaterials in catalysts, medical diagnostics, magnetic materials, cosmetics, coatings/paints/pigments and electronics due to their novel properties such as excellent finite-size effect, optical performance, super paramagnetism and inherent biocompatibility (Hu et al. 2017; Keller et al. 2013). The extensive application of nano-Fe_2O_3 has led to their inevitably release into the aquatic environment during production, usage and disposal. Generally, nano-Fe_2O_3 are considered environmentally friendly, biocompatible, low toxicity, biodegradable and the most stable iron oxide (Bashiri Rezaie and Montazer 2020). Similarly, nano-Fe_2O_3 is recognized to be one of primary components in natural clay minerals in the environment (Braunschweig et al. 2013). Furthermore, many researches have reported that nano-Fe_2O_3 could enhance seed germination, chlorophyll content, root growth in some plants such as *Vigna radiata L.*, *Citrullus lanatus* and *Citrus maxima* (Alidoust and Isoda 2013; Hu et al. 2017; Li et al. 2013; Ren et al. 2011). However, nano-Fe_2O_3 was also considered toxic and obviously decreased the sizes of *Nannochloropsis sp.* and *Isochrysis sp.* due to their agglomerates on the surface of algal cells (Demir et al. 2015).

The widespread occurrence of nano-Fe_2O_3 in diverse water systems may thus alter or affect the fate of coexisting pollutants such as As(V) prevailing in aerobic aquatic environment and its biotransformation caused by microalgae, even their microcystins release. To date, few researches have investigated the impacts of nano-Fe_2O_3 on As bioaccumulation and biotransformation caused by algae in aquatic systems as well as microcystins release. Therefore, the objectives of this study were to explore the effects of nano-Fe_2O_3 on the growth of *M. aeruginosa*, to investigate As(V) toxicity combined with nano-Fe_2O_3, and to analyze As uptake, species, and its subcellular distribution as well as toxins release in *M. aeruginosa* impacted by nano-Fe_2O_3. The obtained findings on how nano-Fe_2O_3 influence As(V) metabolisms in freshwater algae can contribute to better understandings in biogeochemical behavior, aquatic ecosystem health involved

As toxic effects, and remediation of As-contaminated waters, which potentially impacted by nano-Fe_2O_3.

Materials and Methods

Algal culture and nano-Fe_2O_3 characterization

M. aeruginosa was obtained from the Freshwater Algae Culture Collection at the Institute of Hydrobiology (FACHB-905), Chinese Academy of Sciences. And the obtained algae were maintained axenically in Erlenmeyer flasks containing BG11 medium under intermittent illumination (40 W, 16 h light/8 h dark) at 25 ± 1 °C on an orbital incubation (125 rpm). In addition, commercially available nano-Fe_2O_3 (99.5%, 30 nm) were purchased from Macklin Inc. (Shanghai, China). A stock solution of 100.0 g/L nano-Fe_2O_3 was prepared by dispersing nanoparticles in BG11 medium (Millipore, Billerica, MA, USA) and applying sonication for 30 min (50 W/L at 40 kHz) to promote stable suspension. An extra 30-min application of sonication was conducted immediately before dosing. The average hydrodynamic diameter and the zeta potential of nano-Fe_2O_3 were 164.5 ± 11.3 nm and -11.7 ± 0.1 mV, respectively, determined by a Zetasizer Nano ZS90 dynamic light scattering spectrometer (DLS, Malvern Instruments Ltd., UK). Furthermore, As(V) stock solution with concentration of 1.0 g/L was prepared using $Na_3AsO_4 \cdot 12H_2O$ and stocked in dark at 4 °C until usage.

Tolerance of nano-Fe_2O_3 to *M. aeruginosa*

The tested algae of *M. aeruginosa* with an initial cell density approx. 1.0×10^7 cells/mL were transferred to modified BG11 culture (Fe^{3+} free) with one of eight concentrations of nano-Fe_2O_3 (0, 0.1, 0.5, 1, 5, 10, 100 and 1000 mg/L) after centrifugation and twice sterile water washing. All treatments were cultured in the modified BG11 media for 96 h. The algal optical density (OD) at a wavelength of 680 nm, chlorophyll *a* (Chl*a*) and the maximum photosynthetic quantum yield of PSII (Yield) were measured every 24 h. The algal specific growth rate calculated by OD, Chl*a* and Yield were used to determine the stress effects impacted by nano-Fe_2O_3.

As(V) adsorption onto nano-Fe_2O_3 in algal culture medium

It is vital to understand As(V) adsorption on nano-Fe_2O_3 during the biokinetics process. To investigate As(V) adsorption on nano-Fe_2O_3, identical As(V) concentration of 100 μg/L in 100 mL of BG11 with final concentrations of nano-Fe_2O_3 at 0.1, 1 and 5 mg/L suspensions in Erlenmeyer flasks was prepared, respectively. At the period of 3, 5, 7, 9, 11 and 24 h, 5 mL nano-Fe_2O_3 suspensions were collected and filtered

with 0.45 μm syringe filter after centrifugation at 12 000 g for 5 min. Both the supernatant and the original Fe_2O_3 suspension were collected to measure As concentrations, and the adsorption rate (%) of As(V) onto nano-Fe_2O_3 were calculated. Three parallels were set for each treatment.

As(V) toxicity, uptake kinetics and biotransformation

As(V) toxicity response to nano-Fe_2O_3 as iron sources

Taking into account the tolerated data obtained from the above-mentioned experiments of nano-Fe_2O_3 and a similar iron concentration in BG11, appropriate nano-Fe_2O_3 level (5 mg/L) was chosen to conduct As(V) toxicity experiments. A series of As(V) concentrations (from 0 to 100 mg/L) were prepared in the sterile modified media with 5mg/L nano-Fe_2O_3. After 30-min bath ultrasonication, algal cells were then inoculated with initial cell density approx. 1.0×10^7 cells/mL and cultured for 96 h in 250-mL Erlenmeyer flasks. The toxicity of As(V) was expressed as 96 h EC_{50} (effective concentration for 50% of test algae) which were estimated by a sigmoidal dose–response curve equation based on OD, Chl$a$, and Yield (Karadjova et al. 2008). At the end of these experiments, all the amounts of intracellular total As (TAs) and Fe were measured separately from the survival groups that treated with As(V), together with microcystins release in media.

As(V) uptake kinetics and biotransformation affected by nano-Fe_2O_3

$M. aeruginosa$ with initial cell density approx. 1.0×10^7 cells/mL were inoculated and cultured for 5 days, in which As(V) level was fixed at 100 μg/L, and nano-Fe_2O_3 concentration was set as 0, 0.1, 1 and 5 mg/L in modified BG11 media (iron free). After 2, 4, 8, 12, 18, 48, 72, 96 and 120 h of exposure, algal solutions (approx. 20 mL) were sampled to measure intracellular TAs concentration by referring our previous pretreatment methods (Wang et al. 2018a, b). At the end of the experiments (120 h), As species in algal cells and media were all pretreated and detected separately, together with As distribution at subcellular levels for 0 and 5 mg/L nano-Fe2O3 treatments, in order to identify As(V) biotransformation and As subcellular distribution affected by nano-Fe_2O_3.

Regarding the simultaneous As uptake and release, a nonlinear one-compartment model was selected to describe the measured intracellular TAs for each treatment over time according to the following first-order kinetics:

$$[As_{\text{int}}] = k_u/k_e \times [As_{\text{ext}}] \times (1 - e^{k_e t})$$

Herein, As_{int} (μg/g dry weight) refers to the intracellular TAs; As_{ext} (μg/L) refers to the extracellular As concentration

and is assumed as a constant, and t (h) refers to the exposure time; k_u (L/g/h) and k_e (/h) are the rate constants of As uptake and release, respectively (Wang et al. 2014).

According to the kinetic equilibrium of As uptake and release by $M. aeruginosa$, the selected model was applied if $k_e > 0$. The modeling was operated with the program Graph-Pad Prism 8.0. The bioconcentration factor (BCF) of As was calculated as BCF (L/g) = k_u/k_e (Bradac et al. 2009).

Analytical methods

The As subcellular distribution experiments of $M. aeruginosa$ exposed at 100 μg/L As(V) under free and 5 mg/L nano-Fe_2O_3 were conducted according to the differential centrifugation procedure (Siebers et al., 2013). Four fractions were acquired, namely cell walls, chloroplasts, cell organelles and cytoplasmic supernatant. Besides,TAs, As species including As(III), As(V), DMA and MMA in the media and algal cell as well as OD were all detected according to our previous methods used for sample preparation and analysis (Wang et al. 2018a, b, 2014). In brief, the samples we obtained as per the above procedures were further diluted to measure As using inductively coupled plasma mass spectrometry (ICP-MS) and As speciation using high-performance liquid chromatography coupled to inductively coupled plasma-mass spectrometry (HPLC-ICP-MS) (i.e., Agilent LC1100 series coupled with the Agilent ICP-MS 7800a; Instrumental Analysis Center of Huaqiao University). In addition, algal Chl$a$ and yield were observed using an advanced phytoplankton fluorometer (Phyto-PAM, Walz, Germany) after 10 min of dark conditioning of the fresh algae solution (Chalifour and Juneau 2011). The concentrations of microcystins in media were measured using enzyme-linked immunosorbent assay kit (ELISA, purchased from Institute of Hydrobiology, Wuhan, China) according to manufacturer's instructions after membrane filtration. Furthermore, two As genes ($arsC$ and $arsM$) are critically involved in As bioreduction and methylation processes in algae. Herein, the relative gene expression levels of $arsC$ and $arsM$ genes were also quantified in the tested algae at the first day by Real-Time PCR under different nano-Fe_2O_3 treatments (Wang et al. 2019). The detailed quantifications were described in the Supplementary data.

Statistical analysis

All experiments were performed in triplicate, and the results were expressed as their means with corresponding standard deviations (SD). The one-way analysis of variance (ANOVA), t test and Pearson correlation analysis were conducted using IBM SPSS Statistics 23. Significant differences were considered acceptable when $P < 0.05$. Graphics were generated using Origin Pro 2017 and GraphPad Prism 8.0.

Results and Discussion

Algal growth under various nano-Fe₂O₃ levels

The specific growth rate (μ) calculated by OD (μ_{OD}) ranged from 0.00 to 0.37 /d (Fig. 1). Except for the nano-Fe$_2$O$_3$ concentrations of 100 and 1000 mg/L, there were insignificant differences for μ_{OD} with an overall mean of 0.35 ± 0.01 /d and a coefficient of variation (CV) of 0.03 under the other given nano-Fe$_2$O$_3$ levels, while for μ_{Chla} calculated by Chl$a$, it ranged from 0.22 to 0.32 /d. Similar to μ_{OD}, no obvious differences of μ_{Chla} were observed from 0 to 10 mg/L nano-Fe$_2$O$_3$ treatments, with an overall mean of 0.30 ± 0.02 /d and CV of 0.05. The inhibition of Chl$a$ was found at 1000 mg/L nano-Fe$_2$O$_3$ concentrations. Nano-Fe$_2$O$_3$ concentration was found to be significantly correlated with μ_{OD} and μ_{Chla} with the correlation coefficient of -0.801 and -0.723 ($P < 0.01$), respectively. Impliedly, μ_{OD} and μ_{Chla} could greatly respond the effects of *M. aeruginosa* to nano-Fe$_2$O$_3$, and the induced potential algal toxicity was exhibited at more than 100 mg/L concentrations. It was similar to the results that FerMEG12 (pristine flake-like milled Fe(0) nanoparticles (nZVI)) was toxic to *Chlamydomonas sp.* at concentration higher than 50 mg/L (Nguyen et al. 2018). The high algal specific growth rate with paired little CV for μ_{OD} and μ_{Chla} at the concentrations less than 10 mg/L indicated that toxicity and variation in *M. aeruginosa* growth were relatively low affected by nano-Fe$_2$O$_3$ with less than 10 mg/L.

Arsenate toxicity

The As(V) 96 h EC$_{50}$ for *M. aeruginosa* under 5 mg/L nano-Fe$_2$O$_3$ conditions obtained by OD, Chl$a$ and Yield correlated with As concentrations in media and algal cells was found to be well fitted by the sigmoidal dose–response curve with
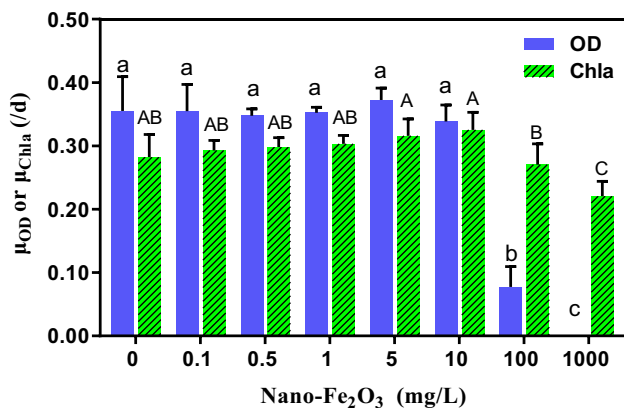
an R^2 range from 0.831 to 0.979 (Fig. S1). *M. aeruginosa* was more sensitive to As(V) coexisting with nano-Fe$_2$O$_3$ as iron sources. The As(V) 96 h EC$_{50}$ calculated from OD and Chl$a$ correlated with As concentrations in media and algal cells was less than four to five orders of magnitude compared with nano-Fe$_2$O$_3$ free, but it was unobvious for Yield (Table 1). Yield as the sensitive indicator of *M. aeruginosa* to As(V) toxicity was changed slightly when iron ion substituted by nano-Fe$_2$O$_3$ in aquatic systems compared with OD and Chl$a$. Nano-Fe$_2$O$_3$ as iron sources of *M. aeruginosa* was considered to remarkably inhibit the algal OD and Chl$a$ under As(V) treatments. This is partly caused by iron deficiency decreasing photosynthetic efficiency due to the participation of iron in Chl$a$ synthesis (Osório et al. 2014). Similar tendency was found for As(V) 96 h EC$_{50}$ with the order of Yield > OD > Chl$a$ under nano-Fe$_2$O$_3$ conditions obtained from As concentrations whether in media or in algal cells. In addition, the intracellular As concentration could reflect As(V) toxicity notably, which reduced the toxicity differences between OD, Chl$a$ and Yield when growth inhibition was plotted against it. Similar observation was reported for *Chlamydomonas reinhardtii* and *Scenedesmus obliquus* (Wang et al. 2013a, b). All 96 h EC$_{50}$ of As(V) obtained from media or intracellular concentrations were more than that of *Chlamydomonas reinhardtii* and *Scenedesmus obliquus* for 48 h EC$_{50}$, which indicated the higher As tolerance of *M. aeruginosa* even impacted by nano-Fe$_2$O$_3$ (Wang et al. 2013a, b).

As(V) concentration was found to be significant negatively correlated with OD, Chl$a$ and Yield, showing the correlation coefficient of -0.937, -0.880 and -0.852 ($P < 0.01$), respectively. Yield was positively correlated with OD and Chl$a$, showing the correlation coefficient of 0.821 and 0.831($P < 0.01$). As the indicator of the ability to transform light energy into chemical energy, Yield could reflect As(V) toxicity well for *M. aeruginosa*, and it was obviously different from the result that Yield could not be a robust indicator of algal growth rate and nutrient status (Kruskopf and Flynn 2006). Meanwhile, Yield become less sensitive indicator compared with OD and Chl$a$ to reflect As(V) toxicity under

Fig. 1 Specific growth rate of *M. aeruginosa* based on OD and Chl$a$ under different nano-Fe$_2$O$_3$ conditions (The different lowercase and uppercase represent significant differences of OD and Chla at 0.05, respectively)

Table 1 D96 h EC$_{50}$ obtained from OD, Chl$a$ and Yield of *M. aeruginosa* under different nano-Fe$_2$O$_3$ conditions

	Fe₂O₃ 0 mg/L	Fe₂O₃ 5 mg/L	
	As in media (µg/L)	As in media (µg/L)	As in algae (µg/g)
OD	5.08×10^9	4.01×10^5	3.67×10^4
R^2	0.974	0.954	0.908
Chla	1.60×10^9	2.43×10^5	2.36×10^4
R^2	0.979	0.840	0831
Yield	3.11×10^6	1.10×10^6	7.01×10^4
R^2	0.916	0.970	0.906

nano-Fe_2O_3 as the iron sources conditions (Table 1), partly caused by its photosynthesis inhibition (Chen et al. 2005).

Intracellular TAs contents after 96 h As(V) exposure were increased with increasing As(V) levels in media, and the maximum iron contents was found at 0.5 mg/L As(V) concentrations and then showed a decline tendency (Fig. 2). The above-mentioned phenomenon confirmed As toxicity on *M. aeruginosa*. Kinetic constants for As uptake under 5 mg/L nano-Fe_2O_3 were calculated by fitting hyperbolic models to the data of As accumulation using the nonlinear regression module (Kahle and Zauke 2002). Arsenic influx can be well described by the Michaelis–Menten equation with R^2 value of 0.995 (Fig. S2). The maximum uptake rate V_{max} (mg/g/d) and the half saturation concentrations (K_m (mg/L)) were 26.12 and 746.10, respectively, which was greater than that of nano-Fe_2O_3 free after 15 days exposure (Wang et al. 2013a, b), but less than V_{max} of *Chlamydomonas reinhardtii* (51.1 mg/g/d) and *Scenedesmus obliquus* (39.5 mg/g/d) from short-term (4 h) experiments under phosphate deficiency conditions and more than that of K_m not exceeding of 0.5 mg/L As(V), respectively (Wang et al. 2013a, b). This indicated that there was high As(V) tolerance of *M. aeruginosa* even under 5 mg/L nano-Fe_2O_3 conditions. Although there was iron free in media, the residual iron in algal cells was still able to maintain its normal growth. Moderate iron supply derived from nano-Fe_2O_3 was found in our study. Furthermore, the depressed iron accumulation in algal cells could reflect As(V) toxicity indirectly (Fig. 2).

Microcystins in media

Microcystin in media under different As(V) concentrations was investigated at the end of the As(V) toxicity experiments (Fig. 3). The average concentration of microcystin in media was 7.26 ± 0.67 mg/L after 96 h algal culture under different As(V) treatments. It was more than 150 times compared
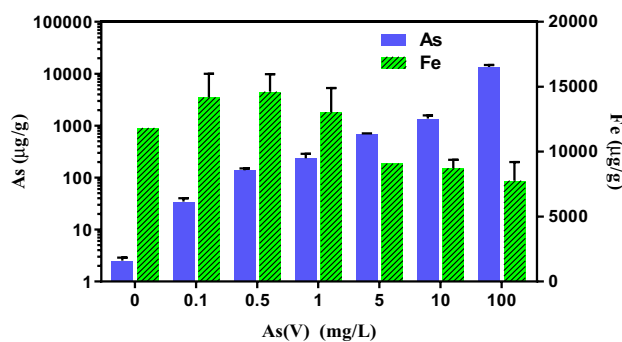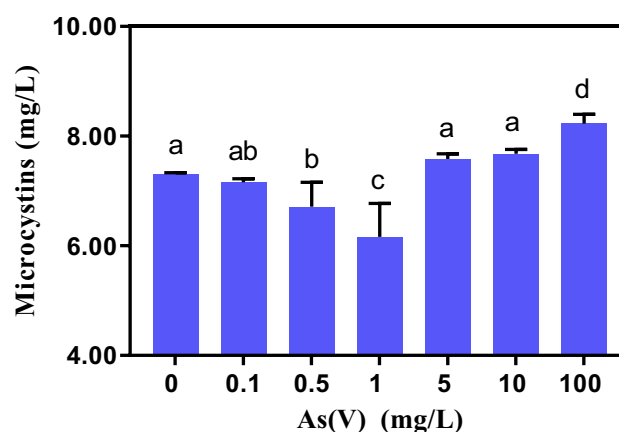

Fig. 3 Microcystins in media of *M. aeruginosa* under different As concentrations affected by nano-Fe_2O_3 of 5 mg/L (The different letters represent significant differences at 0.05)

with previous results of 0.04 mg/L under 1.0×10^7 cells/mL without As(V) stress (Pei et al. 2014), and less than the peak concentration of 29 mg/L found in Lake Oubeira, Algeria (Nasri et al. 2008). These were different from the generally assumption that microcystin did not exceed 0.01 mg/L in cyanobacteria-contaminated water (Cao et al. 2018). In our experiments, microcystin in media was found positively correlated with As concentrations but negatively correlated with intracellular Fe content with the Pearson's correlation coefficient of 0.630 ($P < 0.01$) and -0.554 ($P < 0.05$), respectively. The results were consistent with previous studies that the production of microcystin in *M. aeruginosa* could be accelerated by As(V) in media (Gong et al. 2011). However, it was different from the founding that the intracellular and extracellular quantity of microcystin could be promoted under iron-replete conditions (Wang et al. 2018a, b). Previous studies suggested that iron uptake in *M. aeruginosa* was not congruent with the upregulation of microcystin synthesis (Takaara et al. 2019). Specifically, it can partly be elucidated by the inhibition of As accumulation in algal cells due to iron uptake and thus decreased the abiotic stresses for *M. aeruginosa*. Microcystin concentrations in media decreased first and then increased with increasing As(V) concentrations. The lowest microcystin concentration in media was observed at 1 mg/L As(V) treatments with significantly differences from other As(V) treatments. Gong et al. (Gong et al. 2011) had reported that As(V) at higher than 7.5 mg/L could promote microcystin content in *M. aeruginosa* by inhibiting algal growth, and the lowest microcystin production was found at 0.75 mg/L As(V) treatment. The consistent results illustrated that nano-Fe_2O_3 did not significantly alter microcystin release trends with different As(V) concentrations even though the toxicity of *M. aeruginosa* regulated by nano-Fe_2O_3.

Fig. 2 Intracellular TAs and iron contents in *M. aeruginosa* under different As concentrations affected by 5 mg/L nano-Fe_2O_3. (The vertical coordinate axis for As accumulation is presented by logarithmic)

As(V) uptake kinetics affected by nano-Fe$_2$O$_3$

The TAs concentration in algal cells increased with increasing exposure time for different nano-Fe$_2$O$_3$ treatments (Fig. S3), which were well fitted to the nonlinear one-compartment model with the R^2 (between 0.894 and 0.963) (Fig. S3; Table S1). The calculated k_u for uptake rate constant for As(V) in *M. aeruginosa* under different nano-Fe$_2$O$_3$ treatments ranged from 0.170~0.627 L/g/h. The values of k_u were observed to slightly decreased under lower nano-Fe$_2$O$_3$ (0.1 and 1 mg/L), but prominently increased under 5 mg/L nano-Fe$_2$O$_3$. They were lower than that of *M. aeruginosa* exposed at 10 μM As(V) with k_u from 6.58 to 136.90 L/g/h (Wang et al. 2014). Moreover, it was similar to green algae *Chlamydomonas reinhardtii* (0.40 L/g/h) but more than *Scenedesmus obliquus* (0.09 L/g/h) at 75 μg/L As(V) exposures for 144 h (Wang et al. 2013a, b). In addition, the BCF decreased from 38.46 to 11.40 L/g (Fig. 4), indicating that As accumulated in *M. aeruginosa* was reduced with increasing nano-Fe$_2$O$_3$ in media. However, it was more than *Chlamydomonas reinhardtii* (6.15 L/g) at 75 μg/L As(V) exposures (Wang et al. 2013a, b). Furthermore, the small k_e value for the efflux rate constants (0.005~0.055 /h) suggested a sluggish As release from *M. aeruginosa*, but it increased with nano-Fe$_2$O$_3$ increasing especially for 5 mg/L nano-Fe$_2$O$_3$ which was quintuple of the free nano-Fe$_2$O$_3$ and caused the decrease of BCF. Specifically, k_e values in this study were lower than *Chlamydomonas reinhardtii* (0.065 /h), but similar to our previous study of *M. aeruginosa* (0.017~0.055 /h) when they all exposed at 75 μg/L As(V) conditions (Wang et al. 2013a, b; Wang et al. 2018a, b). Therefore, nano-Fe$_2$O$_3$ as iron sources of *M. aeruginosa* accelerated intracellular As release and decreased intracellular As accumulation. It can be explained by the dilute As(V) concentration in media by As(V) sequestration through high adsorption of nano-Fe$_2$O$_3$ (Fig. S4) (Lin et al. 2019).
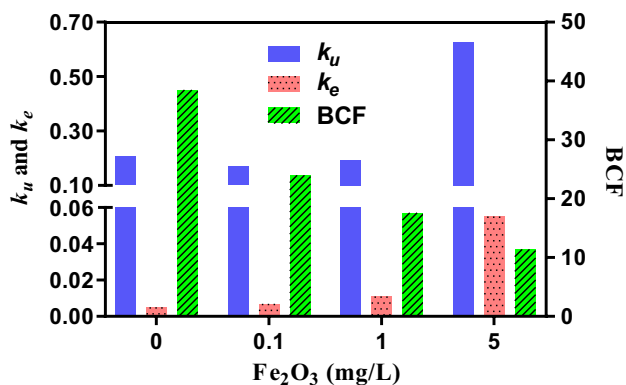

Fig. 4 Estimated As uptake rate constants k_u (L/g/h), intracellular As efflux rate constants K_e (/h) and BCF (L/g) of *M. aeruginosa* under different nano-Fe$_2$O$_3$ level treatments

Furthermore, the rapid As absorption equilibrium in algal cells with nano-Fe$_2$O$_3$ thus decreased As intracellular BCF. Specifically, the BCF of As in *M. aeruginosa* was reduced by 38% under 0.1 mg/L nano-Fe$_2$O$_3$ compared with nano-Fe$_2$O$_3$ free in media. It was different from the result that As BCF in *Daphnia magna* was increased with nano-TiO$_2$ as a positive carrier (Li et al. 2016).

As(V) biotransformation affected by nano-Fe$_2$O$_3$

Except for only As(V) and trace amount of DMA were detected in media under nano-Fe$_2$O$_3$ free treatments, As(III) in media was also determined with less than 1 μg/L concentration under nano-Fe$_2$O$_3$ treatments (Fig. 5). Our previous study shows that *M. aeruginosa* at As(V) exposures was observed with higher organic As (OAs) release rate than that of As(III) (Wang et al. 2013a, b). In this study, relatively high As(III) release in media was decreased with increasing nano-Fe$_2$O$_3$, but OAs concentrations showed opposite tendency (Fig. 5). This indicated that As biotransformation in media was improved to a certain extent by nano-Fe$_2$O$_3$ as iron sources for *M. aeruginosa*. It might be caused by the high conductivity of nano-Fe$_2$O$_3$ and could enhance electron transfer in living organisms to accelerate As(V) biological reduction as well as the subsequent methylation in algal cells and their rapid release to media (Lin et al. 2019). Meanwhile the reported adsorption capacity of nano-Fe$_2$O$_3$ on As(III) was twice than that of As(V) (Tang et al. 2011), which could partly enhance As(III) biotransformation of *M. aeruginosa*. The detailed mechanisms need further investigation.

Although three As species including As(V), As(III) and DMA were all found in algal cells, As(V) remained dominant species with more than 75.0% of intracellular TAs, followed by As(III) with 15.3–24.4% under different nano-Fe$_2$O$_3$ treatments. The intracellular As accumulation decreased with increasing nano-Fe$_2$O$_3$, and significant differences were observed for intracellular As(V) accumulation especially under more than 1 mg/L nano-Fe$_2$O$_3$ treatments (Fig. 5b). This result was consistent with As BCF observed in *M. aeruginosa* under different nano-Fe$_2$O$_3$ treatments, and was different from nano-TiO$_2$ to accelerate As accumulation in *M. aeruginosa* (Luo et al. 2018). Whether in media or in algal cells, As(V) biotransformation (the amount of As(III) and methylated As species) were all improved under 1 mg/L nano-Fe$_2$O$_3$ treatments, which indicated that a suitable nano-Fe$_2$O$_3$ level in aquatic environment could increase As biotransformation. This is supported by the higher relative gene expression levels ($2^{-\Delta CT}$) of *arsC* and *arsM* in elevated nano-Fe$_2$O$_3$ treatments (Fig. S5). Previous studies reported that 5 mg/L nano-Fe$_2$O$_3$ stimulated green algae growth and elevated algal lipid and polyunsaturated fatty acids contents by the dissolved trace ions of nano-Fe$_2$O$_3$ as a trace element for algal growth (He et al. 2017).

Fig. 5 Arsenic species in media and algal cells under different nano-Fe$_2$O$_3$ level treatments (The different letters represent significant differences at 0.05)
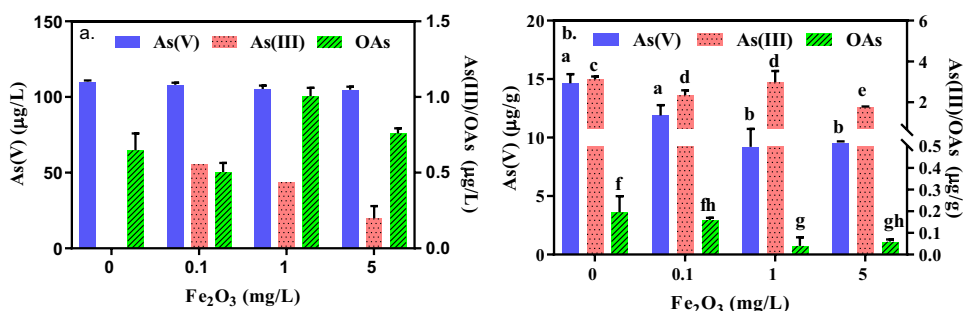
Subcellular distribution of arsenic

From the subcellular distribution of As in algal cells (Fig. 6), we found that As primarily existed in cytoplasmic supernatant of the tested algae with more than 78.0% of TAs. There were insignificant differences of As in cytoplasmic supernatant and chloroplast fractions under both free and 5 mg/L nano-Fe$_2$O$_3$ treatments. More notably, As distributed in cell organelles was increased but decreased in cell walls by nano-Fe$_2$O$_3$ additive, which exhibited significant differences compared with nano-Fe$_2$O$_3$ free (Fig. 6). This indicated that nano-Fe$_2$O$_3$ as As carrier mainly affected As transportation from cell walls to organelles. It might be elucidated by the mild cell wall damage and strong affinity to cell membranes due to the uptake of nano-Fe$_2$O$_3$ for algal cells (Phenrat et al. 2009; Saxena et al. 2020). Meanwhile, chloroplasts were regarded as playing a central role in the cellular iron ion sink of plant cells (Jain and Connolly 2013). Iron deficiency in media might cause nano-Fe$_2$O$_3$ carried with As accumulated in algal organelles and increase As toxic effects (Fig. 2). From these aspects, As biotransformation in algae was then

stimulated potentially by this increased toxic effects of As (Luo et al. 2018).

Environmental implication

In this study, we found nano-Fe$_2$O$_3$ reduce arsenate bioaccumulation in *M. aeruginosa*, but increase arsenic biotransformation (i.e., bioreduction and methylation). It suggests that As ecological risk in *M. aeruginosa* can be lowered by nano-Fe$_2$O$_3$ through its decreased accumulation of arsenic and its subsequent biotransformation into lower toxic species. Taking into account the wide distribution, elevated amount and high As adsorption of nano-Fe$_2$O$_3$ in the environment, the As risks in waters can be mitigated to some extent by nano-Fe$_2$O$_3$. Additionally, this mitigated role cannot lead to release excessive harmful microcystins from the tested algae, supported by the insignificant differences of microcystins release under different As treatments at 5 mg/L nano-Fe$_2$O$_3$ levels compared to other reported values. On the other hand, as the first report on how nano-Fe$_2$O$_3$ influence As metabolisms in freshwater algae, this study provided new insights into how nano-Fe$_2$O$_3$, as one of the components in natural nano-clay minerals, could be used to mitigate the As risks in aquatic environment. The findings would be helpful in the understanding and practical applications of natural clay minerals on algal bioremediation of As-contaminated water. However, various processes and uncertainties of As behaviors are needed to considered in-depth, involving the changes of crystal structures of nano-Fe$_2$O$_3$ and their adsorption of As, other more tested algal species and algal physiological dynamics, and other environmental influencing factors.
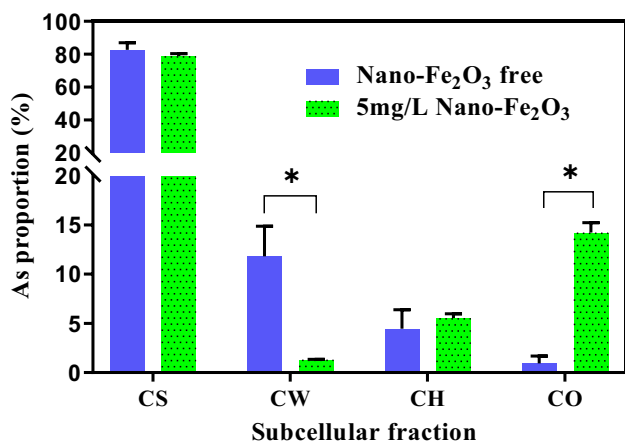
Conclusions

In summary, this study found that nano-Fe$_2$O$_3$ increased As(V) toxicity on *M. aeruginosa*. Meanwhile, nano-Fe$_2$O$_3$ did not significantly alter microcystin release even though the toxicity of *M. aeruginosa* regulated by nano-Fe$_2$O$_3$ under different As(V) concentrations. Due to the efflux rate constants of As increasing with the increase of nano-Fe$_2$O$_3$ and it was more exaggerated than the uptake rate

Fig. 6 Subcellular distribution of As in algal cells under free and 5 mg/L nano-Fe$_2$O$_3$ treatments (* indicates significant differences at 0.05 level). CS, CW, CH and CO represent cytoplasmic supernatant, cell wall, chloroplasts, cell organelles, respectively

constants increasing for 5 mg/L nano-Fe_2O_3 compared with nano-Fe_2O_3 free, the BCF of As was decreased by increasing nano-Fe_2O_3. The reduction of As(V) to As(III) and the subsequently methylation caused by *M. aeruginosa* were observed to be increased with nano-Fe_2O_3 addition, and the optimal As biotransformation was at 1 mg/L nano-Fe_2O_3 conditions. Nano-Fe_2O_3 as iron sources of *M. aeruginosa* regulated As subcellular distribution with declining in cell walls but increasing in cytoplasmic organelles. Accordingly, As accumulation of *M. aeruginosa* was decreased, but its biotransformation was increased due to nano-Fe_2O_3 addition in media. The obtained findings could benefit us to thoroughly understanding how nano-Fe_2O_3 as important natural clay minerals impacts on As biogeochemical behavior and its As removal application of microalgae.

Declarations

Ethics approval The manuscript has not been submitted to more than one journal for simultaneous consideration. No data, text, or theories by others are presented in our manuscript.

Consent to participate Not applicable.

Consent to publish Not applicable.

Competing interests The authors declare no competing interests.

References

Alidoust D, Isoda A (2013) Effect of γFe_2O_3 nanoparticles on photosynthetic characteristic of soybean (Glycine max (L.) Merr.): foliar spray versus soil amendment. Acta Physiol Plant 35(12):3365–3375

BashiriRezaie A, Montazer M (2020) A cleaner and one-step approach for robust coloration of polyester fibers via hydrophobic magnetically recoverable photocatalyst fatty acids/nano iron oxide coating. J Clean Prod 244:118673

Bradac P, Navarro E, Odzak N, Behra R, Sigg L (2009) Kinetics of cadmium accumulation in periphyton under freshwater conditions. Environ Toxicol Chem 28(10):2108–2116

Braunschweig J, Bosch J, Meckenstock RU (2013) Iron oxide nanoparticles in geomicrobiology: From biogeochemistry to bioremediation. New Biotechnol. 30(6):793–802

Cao Q, Steinman AD, Wan X, Xie L (2018) Bioaccumulation of microcystin congeners in soil-plant system and human health risk assessment: A field study from Lake Taihu region of China. Environ Pollut 240:44–50

Chalifour A, Juneau P (2011) Temperature-dependent sensitivity of growth and photosynthesis of *Scenedesmus obliquus*, *Navicula pelliculosa* and two strains of *Microcystis aeruginosa* to the herbicide atrazine. Aquat Toxicol 103(1–2):9–17

Che F, Du M, Yan C (2018) Arsenate biotransformation by *Microcystis aeruginosa* under different nitrogen and phosphorus levels. J Environ Sci (china) 66:41–49

Chen M, Bibby TS, Nield J, Larkum A, Barber J (2005) Iron deficiency induces a chlorophyll d-binding pcb antenna system around photosystem I in *Acaryochloris marina*. Biochim Biophys Acta 1708(3):367–374

Demir V, Ates M, Arslan Z, Camas M, Celik F, Bogatu C et al (2015) Influence of alpha and gamma-iron oxide nanoparticles on marine microalgae species. B Environ Contam Tox 95(6):752–757

Duncan EG, Maher WA, Foster SD (2015) Contribution of arsenic species in unicellular algae to the cycling of arsenic in marine ecosystems. Environ Sci Technol 49(1):33–50

Gong Y, Ao H, Liu B, Wen S, Wang Z, Hu D et al (2011) Effects of inorganic arsenic on growth and microcystin production of a *Microcystis* strain isolated from an algal bloom in Dianchi Lake, China. Chinese Sci Bull 56(22):2337–2342

Hasegawa H, Rahman MA, Kitahara K, Itaya Y, Maki T, Ueda K (2010) Seasonal changes of arsenic speciation in lake waters in relation to eutrophication. Sci Total Environ 408(7):1684–1690

He M, Yan Y, Pei F, Wu M, Gebreluel T, Zou S et al (2017) Improvement on lipid production by *Scenedesmus obliquus* triggered by low dose exposure to nanoparticles. Sci Rep-UK 7(1):15526

Hu J, Guo H, Li J, Gan Q, Wang Y, Xing B (2017) Comparative impacts of iron oxide nanoparticles and ferric ions on the growth of *Citrus maxima*. Environ Pollut 221:199–208

Jain A, Connolly EL (2013) Mitochondrial iron transport and homeostasis in plants. Front Plant Sci 4:348–348

Jia Y, Chen W, Zuo Y, Lin L, Song L (2018) Heavy metal migration and risk transference associated with cyanobacterial blooms in eutrophic freshwater. Sci Total Environ 613–614:1324–1330

Kahle J, Zauke GP (2002) Bioaccumulation of trace metals in the copepod *Calanoides acutus* from the Weddell sea (Antarctica): Comparison of two-compartment and hyperbolic toxicokinetic models. Aquat Toxicol 59(1–2):115–135

Karadjova IB, Slaveykova VI, Tsalev DL (2008) The biouptake and toxicity of arsenic species on the green microalga *Chlorella salina* in seawater. Aquat Toxicol 87(4):264–271

Keller AA, McFerran S, Lazareva A, Suh S (2013) Global life cycle releases of engineered nanomaterials. J Nanopart Res 15(6):1692

Kruskopf M, Flynn KJ (2006) Chlorophyll content and fluorescence responses cannot be used to gauge reliably phytoplankton biomass, nutrient status or growth rate. New Phytol 169(4):841–842

Li J, Chang PR, Huang J, Wang Y, Yuan H, Ren H (2013) Physiological effects of magnetic iron oxide nanoparticles towards watermelon. J Nanosci Nanotechno 13(8):5561–5567

Li M, Luo Z, Yan Y, Wang Z, Chi Q, Yan C et al (2016) Arsenate accumulation, distribution, and toxicity associated with titanium dioxide nanoparticles in *Daphnia magna*. Environ Sci Technol 50(17):9636–9643

Li B, Zhang T, Yang Z (2019) Immobilizing unicellular microalga on pellet-forming filamentous fungus: Can this provide new insights into the remediation of arsenic from contaminated water? Bioresour Technol 284:231–239

Lin J, Hu S, Liu T, Li F, Peng L, Lin Z et al (2019) Coupled kinetics model for microbially mediated arsenic reduction and adsorption/desorption on iron oxides: Role of arsenic desorption induced by microbes. Environ Sci Technol 53(15):8892–8902

Luo Z, Wang Z, Yan Y, Li J, Yan C, Xing B (2018) Titanium dioxide nanoparticles enhance inorganic arsenic bioavailability and methylation in two freshwater algae species. Environ Pollut 238:631–637

Maeda S, Ohki A, Tokuda T, Ohmine M (1990) Transformation of arsenic compounds in a fresh-water food-chain. Appl Organomet Chem 4(3):251–254

Maeda S, Mawatari K, Ohki A, Naka K (1993) Arsenic metabolism in a freshwater food chain: Blue–green alga (Nostoc sp.)→ shrimp (Neocaridina denticulata)→ carp (Cyprinus carpio). Appl Organomet Chem 7(7):467–476

Miyashita S-i, Murota C, Kondo K, Fujiwara S, Tsuzuki M (2016) Arsenic metabolism in cyanobacteria. Environ Chem 13(4):577

Nasri H, El Herry S, Bouaïcha N (2008) First reported case of turtle deaths during a toxic Microcystis spp. Bloom in Lake Oubeira, Algeria. Ecotox Environ Safe 71(2):535–544

Nguyen NHA, Von Moos NR, Slayeykoya VI, Mackenzie K, Meckenstock RU, Thummler S et al (2018) Biological effects of four iron-containing nanoremediation materials on the green alga *Chlamydomonas* sp. Ecotox Environ Safe 154:36–44

Osório J, Osório ML, Correia PJ, de Varennes A, Pestana M (2014) Chlorophyll fluorescence imaging as a tool to understand the impact of iron deficiency and resupply on photosynthetic performance of strawberry plants. Sci Hortic-Amsterdam 165:148–155

Pei HY, Ma CX, Hu WR, Sun F (2014) The behaviors of *Microcystis aeruginosa* cells and extracellular microcystins during chitosan flocculation and flocs storage processes. Bioresour Technol 151:314–322

Phenrat T, Long TC, Lowry GV, Veronesi B (2009) Partial oxidation ("aging") and surface modification decrease the toxicity of nanosized zerovalent iron. Environ Sci Technol 43(1):195–200

Ren H-X, Liu L, Liu C, He S-Y, Huang J, Li J-L et al (2011) Physiological investigation of magnetic iron oxide nanoparticles towards Chinese mung bean. J Biomed Nanotechnol 7(5):677–684

Roy M, Giri AK, Dutta S, Mukherjee P (2015) Integrated phytobial remediation for sustainable management of arsenic in soil and water. Environ Int 75:180–198

Saxena P, Sangela V, Harish (2020) Toxicity evaluation of iron oxide nanoparticles and accumulation by microalgae *Coelastrella terrestris*. Environ Sci Pollut R. 27, 19650-19660

Siebers N, Siangliw M, Tongcumpou Ch (2013) Cadmium uptake and subcellular distribution in rice plants as affected by phosphorus: Soil and hydroponic experiments. J Soil Sci Plant Nut 13(4):833–844

Sulaymon AH, Mohammed AA, Al-Musawi TJ (2013) Competitive biosorption of lead, cadmium, copper, and arsenic ions using algae. Environ Sci Pollut R 20(5):3011–3023

Takaara T, Sasaki S, Fujii M, Ito H, Masago Y, Omura T (2019) Lectin-stimulated cellular iron uptake and toxin generation in the freshwater cyanobacterium *Microcystis aeruginosa*. Harmful Algae 83:25–33

Tang W, Li Q, Gao S, Shang JK (2011) Arsenic (III, V) removal from aqueous solution by ultrafine α-Fe_2O_3 nanoparticles synthesized from solvent thermal method. J Hazard Mater 192(1):131–138

Thomas DJ, Waters SB, Styblo M (2004) Elucidating the pathway for arsenic methylation. Toxicol Appl Pharm 198(3):319–326

Wang NX, Li Y, Deng XH, Miao AJ, Ji R, Yang LY (2013a) Toxicity and bioaccumulation kinetics of arsenate in two freshwater green algae under different phosphate regimes. Water Res 47(7):2497–2506

Wang Z, Luo Z, Yan C (2013b) Accumulation, transformation, and release of inorganic arsenic by the freshwater cyanobacterium *Microcystis aeruginosa*. Environ Sci Pollut R 20(10):7286–7295

Wang Z, Luo Z, Yan C, Che F, Yan Y (2014) Arsenic uptake and depuration kinetics in *Microcystis aeruginosa* under different phosphate regimes. J Hazard Mater 276:393–399

Wang Y, Wang S, Xu P, Liu C, Liu M, Wang Y et al (2015) Review of arsenic speciation, toxicity and metabolism in microalgae. Rev Environ Sci Biotechnol 14(3):427–451

Wang X, Wang P, Wang C, Hu B, Ren L, Yang Y (2018a) Microcystin biosynthesis in *Microcystis aeruginosa*: Indirect regulation by iron variation. Ecotox Environ Safe 148:942–952

Wang Z, Luo Z, Yan C, Rosenfeldt RR, Seitz F, Gui H (2018b) Biokinetics of arsenate accumulation and release in *Microcystis aeruginosa* regulated by common environmental factors: Practical implications for enhanced bioremediation. J Clean Prod 199:112–120

Wang Z, Gui H, Luo Z, Zhen Z, Yan C, Xing B (2019) Dissolved organic phosphorus enhances arsenate bioaccumulation and biotransformation in *Microcystis aeruginosa*. Environmental Pollution 252:1755–1763. https://doi.org/10.1016/j.envpol.2019.06.126

Zeng L, Yan C, Guo J, Zhen Z, Zhao Y, Wang D (2019) Influence of algal blooms decay on arsenic dynamics at the sediment-water interface of a shallow lake. Chemosphere 219:1014–1023

Wang Z, Gui H, Luo Z, Sarakiotia IL, Yan C, Laing GD (2020) Arsenic release: Insights into appropriate disposal of arsenic-loaded algae precipitated from arsenic contaminated water. J Hazard Mater. 384:121249

Yan C, Che F, Zeng L, Wang Z, Du M, Wei Q et al (2016) Spatial and seasonal changes of arsenic species in Lake Taihu in relation to eutrophication. Sci Total Environ 563–564:496–505

Yan Y, Ye J, Xue XM, Zhu YG (2015) Arsenic demethylation by a C.As lyase in Cyanobacterium *Nostoc* sp. PCC 7120. Environ Sci Technol. 49(24):14350–14358

Zhang S, Rensing C, Zhu YG (2014) Cyanobacteria-mediated arsenic redox dynamics is regulated by phosphate in aquatic environments. Environ Sci Technol 48(2):994–1000